American Mineralogist, Volume 89, pages 396–404, 2004

A new rare earth disilicate ($REE_2Si_2O_7$; REE = Dy, Tm, Lu; type-L): Evidence for non-quenchable 10 GPa polymorph with silicon in fivefold trigonal bipyramidal coordination?

MICHAEL E. FLEET* AND XIAOYANG LIU

Department of Earth Sciences, University of Western Ontario, London, Ontario N6A 5B7, Canada

ABSTRACT

A new structure type (L) is reported for disilicates of the middle and heavy rare earth elements (REE) quenched from 10 GPa, 1600–1700 °C. Crystal data are: triclinic, space group $P\bar{1}$, $Z = 6$; $Dy_2Si_2O_7$: $a = 6.5971(3)$, $b = 6.6504(2)$, $c = 18.0582(6)$ Å, $\alpha = 83.791(2)$, $\beta = 88.653(2)$, $\gamma = 88.498(2)°$, $V = 787.2$ Å^3, and $D_x = 6.242$ g/cm^3; $Tm_2Si_2O_7$: $a = 6.5499(2)$, $b = 6.5876(2)$, $c = 17.8916(7)$ Å, $\alpha = 83.828(1)$, $\beta = 88.368(1)$, $\gamma = 88.152(2)°$, $V = 766.9$ Å^3, and $D_x = 6.574$ g/cm^3; $Lu_2Si_2O_7$: $a = 6.5240(2)$, $b = 6.5553(2)$, $c = 17.7909(6)$ Å, $\alpha = 83.977(2)$, $\beta = 88.074(2)$, $\gamma = 87.846(2)°$, $V = 755.8$ Å^3, and $D_x = 6.830$ g/cm^3. The type-L structure comprises linear trisilicate $[Si_3O_{10}]^{8-}$ and orthosilicate $[SiO_4]^{4-}$ ions cross linked by REE^{3+} in one sevenfold and five eightfold coordinated positions (to 3.0 Å), and is assembled from alternating (001) strips of the type-B structure of $REE_2Si_2O_7$ and a sheared structure containing structural elements found in the type-B structure but with Si distributed with 50% occupancy over two face-sharing tetrahedra. The geometry of these half-occupied tetrahedra is consistent with decomposition of a SiO_5 trigonal bipyramid during quenching of the pressure.

INTRODUCTION

Ten different structure types (A-I) have been reported for the single rare earth element (REE) disilicates (Felsche 1970a,b,c, 1971, 1972; Smolin and Shepelev 1970; Smolin et al. 1970; Greis et al. 1991; Dias et al. 1990; Christensen 1994; Christensen and Hazell 1994; Christensen et al. 1997a,b; Fleet and Liu 2000, 2001, 2003; Müller-Bunz and Schleid 2000, 2002). This diversity in structure type is, in part, a consequence of the monotonic decrease in size of the REE^{3+} cation through the lanthanide series. In eight of these structure types (A, C, D, E, F, G, H, and K) the SiO_4 tetrahedra are associated with diorthosilicate $[Si_2O_7]^{6-}$ ions, and the structures essentially represent different ways of packing diorthosilicate anions and REE^{3+} cations in the ratio 1:2. The ninth and tenth structure types are not diorthosilicates. Instead, in the type-B structure, the SiO_4 tetrahedra form a linear trisilicate $[Si_3O_{10}]^{8-}$ ion and a single orthosilicate $[SiO_4]^{4-}$ ion pfu (Felsche 1972; Fleet and Liu 2000, 2003) and, in the type-I structure of $La_2Si_2O_7$, they form a catena-tetrasilicate $[Si_4O_{13}]^{10-}$ ion and two orthosilicate ions pfu (Müller-Bunz and Schleid 2002). The type-B structure has been reported for the disilicates of Eu, Gd, Tb, Dy, Ho, and Er at the lowest temperatures investigated (below 1000–1450 °C) at 1 bar (Felsche 1970a), as well as for the disilicates of Tm, Yb, and Lu at higher pressure (up to 7.0 GPa; Bocquillon et al. 1977). The latter study found that a phase with a new structure type (X; believed to be the silicate analogue of $Er_2Ge_2O_7$; Smolin 1970) replaced the type-C phase at moderate temperature and, in turn, was replaced by the type-B phase at high pressure. Loriers et al. (1977) proposed that this phase transition sequence C → X → B is accompanied by closure of the dihedral (Si-O-Si) bond angle with increase in pressure. This suggestion was supported by the report of the type-K structure for disilicates of Nd, Sm, Eu, and Gd at 10 GPa, 1600–1700 °C (Fleet and Liu 2001), where compression is accomplished mainly by closure of the Si-O-Si bond angle to 123–124°, through rigid body rotation of the two SiO_4 tetrahedra in the diorthosilicate ion.

Silicon in sixfold (octahedral) coordination with O atoms ($^{[6]}$Si) is commonly encountered in high-pressure silicate structures (e.g., Hazen et al. 1996; Fleet 1998), but fivefold-coordinated Si ($^{[5]}$Si) has been reported only for triclinic $CaSi_2O_5$ (Kanzaki et al. 1991; Angel et al. 1996), in a square-pyramidal environment formed by distortion of a SiO_6 octahedron on quenching a high-pressure monoclinic phase with the titanite ($CaTiSiO_5$) structure (Angel 1997; Warren et al. 1999), and in K-silicate glass quenched from high pressure (Stebbins and McMillan 1989). There has also been a theoretical prediction of square-pyramidal SiO_5 pentahedra in a new high-pressure phase of silica (SiO_2) (Wentzcovitch et al. 1998), and a nonquenchable SiO_5 trigonal bipyramid was a possible explanation for face-sharing Si(Al) tetrahedra of 50% occupancy in the high-pressure phase $CaAl_4Si_2O_{11}$ (Gautron et al. 1997, 1999). In contrast, fivefold-coordinated Si with trigonal bipyramidal geometry for the SiX_5 group is commonly encountered in organosilane and organosilicate structures (e.g., Turley and Boer 1968; Tacke et al. 2001), and organosilicates with SiO_5 trigonal bipyramids have been reported recently as well (Tacke et al. 1999, 2000). In this paper, we report a new REE disilicate structure (type L) for middle and heavy REE disilicates ($Dy_2Si_2O_7$, $Tm_2Si_2O_7$, and $Lu_2Si_2O_7$) quenched from high pressure. The new structure is analogous to the type-B structure, having SiO_4 tetrahedra as linear trisilicate $[Si_3O_{10}]^{8-}$ and orthosilicate $[SiO_4]^{4-}$ ions, but has one in six Si atoms distributed with 50% occupancy over two face-sharing tetrahedral positions in a manner consistent with decomposition of a SiO_5 trigonal bipyramid. A preliminary report of type-L $Dy_2Si_2O_7$ was given in Liu and Fleet (2002).

* E-mail: mfleet@uwo.ca

EXPERIMENTAL METHODS

Single crystals of REE disilicates ($REE_2Si_2O_7$; REE = Dy, Tm, Lu) were synthesized using the MA6/8 superpress at the University of Alberta, Edmonton. A typical synthesis experiment (Table 1) was run in a Pt capsule within a 14M assembly using a $LaCrO_3$ furnace (Walter et al. 1995), and monitored with a $W_{95}Re_5$-$W_{74}Re_{26}$ thermocouple. All furnace parts were previously fired at 1000 °C in air. The capsule was not dried before welding shut and the assembly with capsule inserted was stored at 110 °C prior to the experiment. Starting materials were high purity REE_2O_3 and amorphous silica (Aldrich Chemical Co.) mixed in stoichiometric proportion and pre-reacted at 950 °C for 2 hours in Pt crucibles; H_2O was added for the synthesis of $Tm_2Si_2O_7$ and $Lu_2Si_2O_7$. The temperature was quenched by switching off the power to the furnace at the experimental pressure; the quench rate at high pressure was estimated to be about 1000 °C/s. The products of the opened capsules consisted of a few single-crystal fragments of $REE_2Si_2O_7$ type-L that were generally tablet shaped and ranged up to 150 µm in maximum diameter. A second synthesis experiment for $Dy_2Si_2O_7$ (no. 3164) at 10 GPa, 1700 °C and 12 hours duration also yielded crystals of type-L. Overall, we attempted synthesis of a broad selection of middle- and heavy-REE disilicates at 10 GPa, 1600 and 1700 °C, for both "dry" and with added H_2O bulk compositions. Some of these additional experiments did result in crystals of type-L disilicates, but most of them yielded unreacted or incompletely reacted starting material.

Crystals of type-L $Ho_2Si_2O_7$ and $Tm_2Si_2O_7$ were also synthesized in experiments at 4.0 GPa using an end-loaded piston-cylinder apparatus. Similarly to the procedure in Fleet and Liu (2003), all furnace parts were previously fired at 1000 ºC in air. Pressure was calibrated from melting of dry NaCl at 1050 °C (Bohlen 1984) and the transformation of quartz to coesite at 500 °C (Bohlen and Boettcher 1982). The temperature was measured by inserting a Pt-Pt90%Rh10% thermocouple into the high-pressure cell. The starting composition, with 5 wt% H_2O added, was encapsulated in a sealed platinum tube with a diameter of 5 mm and a height of 12 mm, which was separated by MgO powder from a graphite tube. The experiments were of 5 hours duration and were quenched at pressure by switching off the furnace. Twinned crystals of type-L structure resulted for experiments with $Ho_2O_3 + 2SiO_2$ at 1450 °C (experiment PC11) and $Tm_2O_3 + 2SiO_2$ at 1250 (PC12) and 1450 °C (PC14).

The experimental products were characterized as single-phase type-L REE disilicates by petrographic optical microscopy, single-grain Gandolfi and powder X-ray diffraction, single-crystal X-ray diffraction, and, for experiments no. 3136 and no. 3201, by electron probe microanalysis (EPMA), using a JEOL 8600 Superprobe. The electron probe microanalyzer was operated at an accelerating voltage of 20 kV, a beam current of 15 nA, a beam diameter of 2 µm, 20 s counts, and $DyPO_4$, $LuPO_4$, and albite ($NaAlSi_3O_8$) as standards, and the measurements were reduced using the Love-Scott model (Sewell et al. 1985). Crystal fragments of the Dy disilicate (no. 3136) gave a composition of Dy_2O_3 74.6(4) and SiO_2 23.0(2) wt%, corresponding to a formula of $Dy_{2.09}Si_2O_7$. The small discrepancy with the ideal formula was interpreted as an artifact of the analytical method used, and particularly to the difficulty in calibrating EPMA for a large amount of a heavy metal. EPMA of the Lu disilicate (no. 3201) resulted in a composition of Lu_2O_3 76.4(3) and SiO_2 24.3(1) wt% and a formula of $Lu_{1.94}Si_{2.04}O_7$, suggesting a small deficiency in Lu relative to the ideal stoichiometry. Nonstoichiometry is also indicated by the low refined occupancy [0.906(4)] of the Lu4 position (Table 2).

Single-crystal fragments were prepared by trimming tablet-shaped grains of the disilicates with a scalpel blade; these were subsequently evaluated for X-ray structure analysis by optical petrography and X-ray precession photography. Single-crystal measurements were made at room temperature and pressure with a Nonius Kappa CCD diffractometer and graphite-monochromatized Mo$K\alpha$ X-radiation (50 kV, 32 mA, λ = 0.7107 Å). The COLLECT Nonius software was used for unit-cell refinement and data collection. The reflection data were processed with SORTAV-COLLECT, using an empirical procedure for absorption correction, and SHELXTL/PC (Siemens 1993) was used for structure determination. Structure refinements were made with LINEX77 (Coppens 1997a), using the nominal compositions for $Dy_2Si_2O_7$, $Tm_2Si_2O_7$, and $Lu_2Si_2O_7$. Scattering factors for neutral atomic species and values of f' and f'' were taken, respectively, from Tables 2.2A and 2.3.1 of the *International Tables for X-ray Crystallography* (Ibers and Hamilton 1974). Relevant experimental details are given in Table 1, final parameters in Table 2, selected bond distances and angles in Table 3, observed and calculated structure factors in Table 4[1], and selected views of the type-L structure of $Dy_2Si_2O_7$ in Figures 1, 2, and 3.

TABLE 1. Experimental details

	$Dy_2Si_2O_7$	$Tm_2Si_2O_7$	$Lu_2Si_2O_7$
experiment	no. 3136	no. 3245	no. 3201
H_2O (wt%)	dry: 110°C	5.9	5
temperature* (°C)	1600	1700	1600
pressure* (GPa)	10	10	10
time† (h)	24	12	24
crystal	xt354	xt369	xt364
crystal size ($mm^3 \times 10^3$)	0.08	0.25	0.1
crystal shape	prism	equant	tablet
µ‡ (cm^{-1})	287	361.2	413.5
a (Å) ($P\bar{1}$)	6.5971(3)	6.5499(2)	6.5240(2)
b (Å)	6.6504(2)	6.5876(2)	6.5553(2)
c (Å)	18.0582(6)	17.8916(7)	17.7909(6)
α (°)	83.791(2)	83.828(1)	83.977(2)
β (°)	88.653(2)	88.368(1)	88.074(2)
γ (°)	88.498(2)	88.152(2)	87.846(2)
D_x (g/cm^3)	6.242	6.574	6.83
reflections-unique	6909	4467	4402
-number with ($I<3\sigma_I$)	2475	1803	2376
R_{int}‡	0.037	0.036	0.038
refined parameters	308	199	199
R§	0.043	0.039	0.04
wR§	0.042	0.035	0.034
σ§	1.026	0.942	0.724
extinction (x10^4)	0.94(2)	0.288(9)	0.205(7)
Δρ# ($eÅ^{-3}$) (+)	2.95	2.4	2.62
(–)	2.53	2.89	2.38

* Temperature and pressure of crystal synthesis; XRD measurements were made at room temperature and pressure.
† Time at final temperature.
‡ µ is linear absorption coefficient; R_{int} is residual index for intensities of equivalent reflections .
§ Least-squares refinement parameters: *R* is residual index; *wR* is weighted residual index; σ is goodness-of-fit.
# Δρ is residual electron density.

[1]For a copy of Table 4, document item AM-04-056, contact the Business Office of the Mineralogical Society of America (see inside front cover of recent issue) for price information. Deposit items may also be available on the American Mineralogist web site at http://www.minsocam.org.

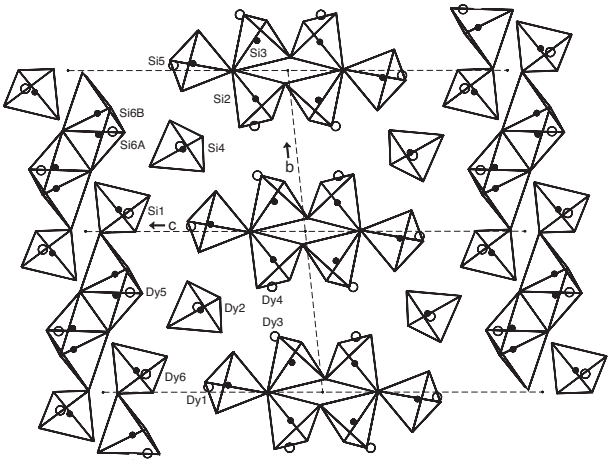

FIGURE 1. Polyhedral representation of the type-L structure of $Dy_2Si_2O_7$ locating Dy (open circles) and Si (small full circles) positions. The linear trisilicate $[Si_3O_{10}]^{8-}$ and orthosilicate $[Si4O_4]^{4-}$ ions form the (001) strip of type-B structure, and the chain of corner-, face-, and edge-shared SiO_4 tetrahedra form the interspersed strip of disordered sheared structure; [100] projection; drawn with *ORTEP*3 (Farrugia 1999).

TABLE 2. Atomic coordinates and isotropic displacement parameters (A^2) $U_{eq} = (1/3)\,\Sigma_i\Sigma_j\, U^{ij}\, a^i a^j\, \mathbf{a}_i.\mathbf{a}_j$

Position	Occupancy	*x*	*y*	*z*	U,U_{eq}
		$Dy_2Si_2O_7$			
Dy1	1	0.54669(6)	0.03160(5)	0.25884(2)	0.0077(1)
Dy2	1	0.81887(6)	0.52945(5)	0.26374(2)	0.0082(1)
Dy3	1	0.61495(5)	0.34691(5)	0.09507(2)	0.0067(1)
Dy4	1	0.12017(6)	0.65444(6)	0.08928(2)	0.0098(1)
Dy5	1	0.42509(7)	0.62047(6)	0.41389(2)	0.0152(1)
Dy6	1	0.13288(7)	0.11258(6)	0.39816(2)	0.0187(1)
Si1	1	0.6517(3)	0.1347(3)	0.4189(1)	0.0066(4)
Si2	1	0.6358(3)	0.8230(3)	0.0801(1)	0.0051(4)
Si3	1	0.1232(3)	0.1843(3)	0.0626(1)	0.0069(4)
Si4	1	0.3383(3)	0.5108(3)	0.2579(1)	0.0060(4)
Si5	1	0.0052(3)	0.0437(3)	0.2138(1)	0.0059(4)
Si6A	0.5	0.9552(7)	0.6024(7)	0.4469(2)	0.012(1)
Si6B	0.5	0.8999(7)	0.7340(7)	0.4436(2)	0.009(1)
O1	1	0.2180(8)	0.0811(8)	0.9909(3)	0.012(1)
O2	1	0.4558(8)	0.6962(7)	0.0475(3)	0.009(1)
O3	1	0.9214(8)	0.3094(8)	0.0356(3)	0.012(1)
O4	1	0.2727(8)	0.3464(7)	0.0864(3)	0.008(1)
O5	1	0.7757(8)	0.6452(8)	0.1244(3)	0.011(1)
O6	1	0.5655(8)	0.0042(8)	0.1264(3)	0.010(1)
O7	1	0.0864(7)	0.9937(7)	0.1264(2)	0.006(1)
O8	1	0.8685(8)	0.2497(7)	0.1938(3)	0.011(1)
O9	1	0.1447(8)	0.5875(8)	0.2103(3)	0.010(1)
O10	1	0.5023(8)	0.3721(7)	0.2159(3)	0.008(1)
O11	1	0.8518(8)	0.8701(7)	0.2472(2)	0.008(1)
O12	1	0.1965(8)	0.0624(8)	0.2655(3)	0.011(1)
O13	1	0.4865(8)	0.6897(7)	0.2808(3)	0.008(1)
O14	1	0.7799(9)	0.2223(8)	0.3451(3)	0.013(1)
O15	1	0.2632(9)	0.4022(8)	0.3383(3)	0.019(1)
O16	1	0.7705(10)	0.6148(10)	0.3867(3)	0.027(2)
O17	1	0.4709(8)	0.9977(7)	0.3871(3)	0.010(1)
O18	1	0.1182(9)	0.7716(9)	0.4118(3)	0.021(1)
O19	1	0.8152(10)	0.9907(10)	0.4673(3)	0.026(2)
O20	1	0.5489(8)	0.3046(8)	0.4668(3)	0.012(1)
O21	1	0.1184(12)	0.3755(8)	0.4726(3)	0.031(2)
		$Tm_2Si_2O_7$			
Tm1	0.980(4)	0.54372(7)	0.03118(7)	0.25872(3)	0.0063(2)
Tm2	0.991(4)	0.81604(7)	0.53057(7)	0.26274(3)	0.0071(2)
Tm3	0.985(4)	0.61586(7)	0.34733(7)	0.09585(3)	0.0059(2)
Tm4	0.971(4)	0.12118(7)	0.65008(8)	0.09028(3)	0.0072(2)
Tm5	0.984(4)	0.42926(8)	0.62039(8)	0.41346(3)	0.0134(2)
Tm6	0.991(4)	0.13580(8)	0.11216(8)	0.39754(3)	0.0181(2)
Si1	1	0.6548(4)	0.1374(4)	0.4190(2)	0.0057(7)
Si2	1	0.6343(4)	0.8231(4)	0.0813(2)	0.0055(7)
Si3	1	0.1231(4)	0.1822(4)	0.0621(2)	0.0063(7)
Si4	1	0.3375(4)	0.5103(4)	0.2587(2)	0.0051(7)
Si5	1	0.0042(4)	0.0423(4)	0.2145(2)	0.0049(7)
Si6A	0.5	0.9570(8)	0.6017(9)	0.4456(4)	0.006(1)*
Si6B	0.5	0.9040(8)	0.7332(9)	0.4440(4)	0.005(1)*
O1	1	0.2214(9)	0.0779(10)	0.9890(4)	0.010(2)*
O2	1	0.4554(10)	0.6923(10)	0.0505(4)	0.012(2)*
O3	1	0.9170(10)	0.3108(10)	0.0354(4)	0.010(2)*
O4	1	0.2724(10)	0.3463(10)	0.0865(4)	0.008(2)*
O5	1	0.7781(9)	0.6458(10)	0.1245(4)	0.007(2)*
O6	1	0.5651(10)	0.0093(10)	0.1268(4)	0.009(2)*
O7	1	0.0873(9)	0.9875(10)	0.1270(4)	0.006(2)*
O8	1	0.8698(9)	0.2519(10)	0.1923(4)	0.009(2)*
O9	1	0.1419(9)	0.5880(10)	0.2108(4)	0.009(2)*
O10	1	0.5044(9)	0.3721(10)	0.2149(4)	0.006(2)*
O11	1	0.8486(9)	0.8711(9)	0.2495(4)	0.005(2)*
O12	1	0.1963(9)	0.0605(10)	0.2658(4)	0.007(2)*
O13	1	0.4851(10)	0.6949(10)	0.2802(4)	0.013(2)*
O14	1	0.7893(10)	0.2254(11)	0.3442(5)	0.017(2)*
O15	1	0.2745(9)	0.3989(10)	0.3412(4)	0.009(2)*
O16	1	0.7721(11)	0.6162(11)	0.3857(5)	0.019(2)*
O17	1	0.4763(9)	0.9992(10)	0.3867(4)	0.005(2)*
O18	1	0.1251(10)	0.7757(10)	0.4095(4)	0.013(2)*
O19	1	0.8166(11)	0.9895(11)	0.4674(5)	0.024(2)*
O20	1	0.5524(9)	0.3075(10)	0.4678(4)	0.007(2)*
O21	1	0.1139(11)	0.3725(12)	0.4709(5)	0.025(2)*
		$Lu_2Si_2O_7$			
Lu1	0.961(4)	0.54296(8)	0.03148(9)	0.25839(3)	0.0097(2)
Lu2	0.972(4)	0.81377(8)	0.53185(9)	0.26105(3)	0.0093(2)
Lu3	0.967(4)	0.61557(8)	0.34637(9)	0.09551(3)	0.0089(2)
Lu4	0.906(4)	0.12070(9)	0.64583(10)	0.09097(3)	0.0095(2)
Lu5	0.970(4)	0.43223(9)	0.62021(9)	0.41313(3)	0.0158(2)
Lu6	0.969(4)	0.13704(9)	0.11235(10)	0.39622(3)	0.0206(2)
Si1	1	0.6551(5)	0.1397(6)	0.4184(2)	0.0100(9)
Si2	1	0.6311(5)	0.8232(5)	0.0819(2)	0.0088(9)
Si3	1	0.1222(5)	0.1810(6)	0.0614(2)	0.0101(9)
Si4	1	0.3385(5)	0.5109(6)	0.2592(2)	0.0093(9)
Si5	1	0.0036(5)	0.0412(5)	0.2134(2)	0.0090(9)
Si6A	0.5	0.9604(10)	0.6024(12)	0.4446(4)	0.009(2)*
Si6B	0.5	0.9079(11)	0.7330(2)	0.4440(4)	0.010(2)*
O1	1	0.2317(11)	0.0766(12)	0.9895(4)	0.012(2)*
O2	1	0.4487(12)	0.6900(12)	0.0520(4)	0.015(2)*
O3	1	0.9193(11)	0.3095(12)	0.0321(4)	0.010(2)*
O4	1	0.2712(11)	0.3438(12)	0.0876(4)	0.008(2)*
O5	1	0.7766(11)	0.6421(12)	0.1244(4)	0.011(2)*
O6	1	0.5620(11)	0.0081(12)	0.1292(4)	0.013(2)*
O7	1	0.0891(11)	0.9825(12)	0.1257(4)	0.008(2)*
O8	1	0.8708(11)	0.2519(12)	0.1913(4)	0.012(2)*
O9	1	0.1372(11)	0.5855(12)	0.2129(4)	0.011(2)*
O10	1	0.5045(11)	0.3761(12)	0.2147(4)	0.008(2)*
O11	1	0.8474(11)	0.8725(12)	0.2496(4)	0.007(2)*
O12	1	0.1951(11)	0.0605(13)	0.2660(4)	0.013(2)*
O13	1	0.4843(11)	0.6956(12)	0.2796(4)	0.013(2)*
O14	1	0.7914(13)	0.2252(14)	0.3450(5)	0.030(2)*
O15	1	0.2785(12)	0.3994(13)	0.3405(5)	0.021(2)*
O16	1	0.7747(12)	0.6145(14)	0.3856(5)	0.023(2)*
O17	1	0.4791(11)	0.9994(12)	0.3863(4)	0.009(2)*
O18	1	0.1318(12)	0.7728(13)	0.4089(4)	0.016(2)*
O19	1	0.8158(12)	0.9910(14)	0.4675(5)	0.022(2)*
O20	1	0.5502(11)	0.3159(12)	0.4667(4)	0.010(2)*
O21	1	0.1095(14)	0.3742(15)	0.4684(5)	0.036(3)*

* Isotropic refinement.

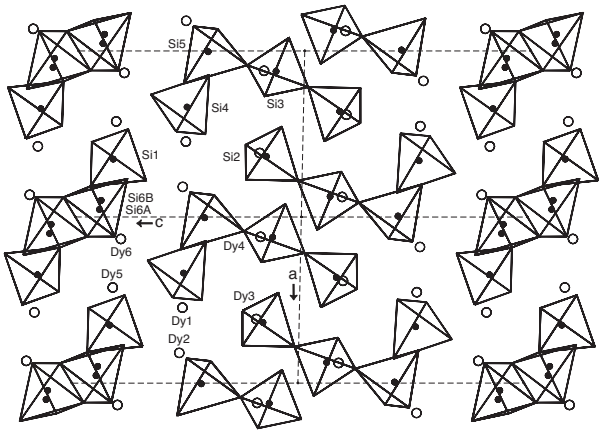

◀ **FIGURE 2.** Polyhedral representation of the type-L structure of $Dy_2Si_2O_7$ viewed in [010] projection; see the Figure 1 caption for further explanation; drawn with *ORTEP*3 (Farrugia 1999).

DISCUSSION

Type-L structure

The silicate topology of the type-B structure of the single REE disilicates is a one-to-one mixture of linear trisilicate $[Si_3O_{10}]^{8-}$ and orthosilicate $[SiO_4]^{4-}$ ions (Fleet and Liu 2003). The type-L structure (Tables 2 and 3; Figs. 1–3) comprises alternating (001) strips of type-B-like structure and a disordered sheared structure containing structural elements found in the type-B structure.

The (010) strip of sheared structure that is interspersed with

TABLE 3. Selected bond distances (Å) and angles (°)

Bond/angle	$Dy_2Si_2O_7$	$Tm_2Si_2O_7$	$Lu_2Si_2O_7$
REE1-O6	2.419(4)	2.380(8)	2.318(7)
REE1-O8	2.769(5)	2.788(6)	2.790(8)
REE1-O10	2.326(5)	2.307(6)	2.318(8)
REE1-O11	2.273(5)	2.239(6)	2.217(7)
REE1-O12	2.315(5)	2.279(6)	2.271(7)
REE1-O13	2.309(5)	2.251(7)	2.240(8)
REE1-O14	2.654(5)	2.694(8)	2.710(8)
REE1-O17	2.347(5)	2.308(7)	2.289(7)
	2.426	2.406	2.394
REE2-O5	2.571(5)	2.524(7)	2.480(7)
REE2-O8	2.370(4)	2.348(7)	2.333(7)
REE2-O9	2.360(5)	2.329(6)	2.276(8)
REE2-O10	2.568(5)	2.534(6)	2.497(7)
REE2-O11a	2.268(5)	2.246(6)	2.239(8)
REE2-O13a	2.440(5)	2.419(6)	2.395(7)
REE2-O14	2.399(5)	2.361(7)	2.381(10)
REE2-O16	2.363(5)	2.336(8)	2.339(8)
	2.418	2.387	2.367
REE3-O2	2.592(5)	2.535(7)	2.523(8)
REE3-O2b	2.674(4)	2.714(8)	2.707(7)
REE3-O3	2.287(5)	2.241(6)	2.264(7)
REE3-O4	2.267(5)	2.261(6)	2.256(7)
REE3-O5	2.388(5)	2.375(6)	2.351(8)
REE3-O6	2.318(5)	2.269(7)	2.273(8)
REE3-O8	2.496(5)	2.450(7)	2.440(7)
REE3-O10	2.311(4)	2.252(7)	2.243(7)
	2.417	2.387	2.382
REE4-O2	2.336(5)	2.299(6)	2.247(8)
REE4-O3c	2.265(5)	2.256(8)	2.202(7)
REE4-O3b	2.936(5)	2.913(7)	2.912(7)
REE4-O4	2.264(5)	2.211(6)	2.183(7)
REE4-O5c	2.345(5)	2.313(6)	2.303(7)
REE4-O7	2.425(4)	2.387(6)	2.353(7)
REE4-O9c	2.191(5)	2.158(8)	2.170(7)
	2.395	2.362	2.339
REE5-O13a	2.424(5)	2.403(8)	2.391(8)
REE5-O15	2.385(5)	2.324(7)	2.315(8)
REE5-O16	2.320(7)	2.286(7)	2.271(8)
REE5-O17a	2.527(5)	2.517(6)	2.509(8)
REE5-O18	2.236(6)	2.209(6)	2.166(7)
REE5-O20	2.275(4)	2.233(7)	2.228(7)
REE5-O20d	2.346(6)	2.313(7)	2.240(8)
REE5-O21	2.752(7)	2.779(7)	2.790(10)
	2.408	2.383	2.364
REE6-O12	2.479(4)	2.436(7)	2.392(7)
REE6-O14c	2.596(6)	2.546(7)	2.517(8)
REE6-O15	2.282(5)	2.249(7)	2.248(9)
REE6-O17	2.349(5)	2.337(6)	2.332(7)
REE6-O18e	2.259(6)	2.207(7)	2.215(9)
REE6-O19	2.481(5)	2.464(9)	2.474(8)
REE6-O19f	2.521(6)	2.516(7)	2.523(9)
REE6-O21	2.317(5)	2.268(8)	2.248(9)
	2.411	2.378	2.369
Si1-O14	1.624(5)	1.644(8)	1.618(10)
Si1-O17	1.669(5)	1.659(7)	1.651(8)
Si1-O19g	1.629(7)	1.620(9)	1.617(9)
Si1-O20	1.621(5)	1.611(7)	1.628(7)
	1.636	1.634	1.629
Si2-O1	1.667(5)	1.642(7)	1.625(9)
Si2-O2	1.631(5)	1.620(7)	1.637(8)
Si2-O5	1.632(6)	1.621(7)	1.630(8)
Si2-O6a	1.592(5)	1.591(7)	1.590(8)
	1.63	1.618	1.62
Si3-O1b	1.634(5)	1.647(8)	1.643(8)
Si3-O3c	1.609(6)	1.626(7)	1.614(8)
Si3-O4	1.579(5)	1.584(7)	1.585(8)
Si3-O7e	1.637(5)	1.654(7)	1.655(9)
	1.615	1.628	1.624
Si4-O9c	1.598(6)	1.602(8)	1.606(8)
Si4-O10	1.630(5)	1.637(7)	1.612(7)
Si4-O13a	1.652(5)	1.661(7)	1.645(8)
Si4-O15	1.623(5)	1.625(8)	1.595(10)
	1.626	1.631	1.614
Si5-O7h	1.718(4)	1.713(8)	1.715(7)
Si5-O8	1.632(6)	1.632(7)	1.622(8)
Si5-O11	1.613(5)	1.609(7)	1.603(9)
Si5-O12i	1.603(5)	1.594(8)	1.603(8)
	1.642	1.637	1.636
Si6A-O16	1.647(8)	1.635(10)	1.624(10)
Si6A-O18i	1.644(7)	1.682(9)	1.673(12)
Si6A-O21d	1.542(6)	1.576(11)	1.620(11)
Si6A-O21i	1.854(8)	1.822(10)	1.775(12)
	1.672	1.679	1.673
Si6B-O16	1.633(7)	1.643(10)	1.648(10)
Si6B-O18i	1.554(7)	1.580(8)	1.589(11)
Si6B-O19d	1.872(8)	1.852(9)	1.858(11)
Si6B-O21d	1.609(7)	1.607(11)	1.643(12)
	1.667	1.671	1.685
O16-Si6A-O18i	105.1(4)	105.2(5)	106.9(6)
O16-Si6A-O21d	113.6(5)	114.7(5)	115.2(6)
O16-Si6A-O21i	125.0(4)	124.3(5)	122.6(6)
O18i-Si6A-O21d	115.2(4)	113.7(5)	113.8(6)
O18i-Si6A-O21i	103.1(4)	104.2(4)	104.3(5)
O21d-Si6A-O21i	94.9(4)	94.5(5)	93.5(6)
Si6B-Si6A-O21i	162.4(6)	161.5(8)	161.9(8)
O16-Si6B-O18i	110.1(4)	109.7(5)	109.8(6)
O16-Si6B-O19d	120.8(4)	119.4(5)	118.7(5)
O16-Si6B-O21d	110.8(4)	112.5(5)	112.6(7)
O18i-Si6B-O19d	102.6(4)	102.1(5)	103.3(6)
O18i-Si6B-O21d	116.5(5)	117.8(5)	117.2(6)
O19d-Si6B-O21d	95.7(3)	94.8(5)	94.6(5)
Si6A-Si6B-O19d	162.4(5)	164.7(8)	166.0(8) 7

Notes: a = *x*, 1 + *y*, *z*; b = 1 – *x*, 1 – *y*, - *z*; c = *x* – 1, *y*, *z*; d = 1 – *x*, 1 – *y*, 1 – *z*; e = *x*, *y* – 1, *z*; f = - *x*, - *y*, 1 – *z*; g = 1 – *x*, - *y*, 1 – *z*; h = 1 + *x*, *y* – 1, *z*; i = 1 + *x*, *y*, *z*.

the strip of type-B structure also appears to be formed of a linear trisilicate ion and an isolated SiO_4 tetrahedron interconnected by Dy atoms in the locally ordered type-L structure. In all three refined type-L structures ($Dy_2Si_2O_7$, $Tm_2Si_2O_7$, and $Lu_2Si_2O_7$; Table 2) there are two Si positions with half occupancy (Si6A and Si6B) which result in all of the SiO_4 tetrahedra being seemingly linked in a single linear six-membered chain of Si1 cornered-linked to Si6B face-linked to Si6A edged-linked to Si6A faced-linked to Si6B corner-linked to Si1 (Fig. 4a). The silicate chains are cross linked by Dy5 and Dy6. Recognizing that Si6A and Si6B are disordered and that face-shared SiO_4 tetrahedra are an unstable combination in the pressure range investigated, this six-membered chain is logically reduced to the two ordered combinations of linear trisilicate ion and isolated SiO_4 tetrahedron shown in Figures 4b and 4c.

Overall, there are interpreted to be two non-equivalent linear trisilicate $[Si_3O_{10}]^{8-}$ and two non-equivalent orthosilicate $[SiO_4]^{4-}$ ions in the type-L structure. The REE^{3+} cations are accommodated in irregular polyhedra: five in eightfold and one in sevenfold coordination to 3.0 Å. As in the type-B structure, there are some discrepancies in the calculated bond valence sums of the O atoms (values for $Dy_2Si_2O_7$ are given in Table 5); O1, O2, O8, O12, O14, and O16 being underbonded and O3, O4, O9, and O18 overbonded. Si6A and Si6B are seemingly underbonded as well due to the anomalously long distances to the axial O atoms of the enclosing trigonal bipyramid, which are Si6A-O21 = 1.854 Å and Si6B-O19 = 1.872 Å. The data in Table 5 were calculated with the bond valence parameters of Brese and O'Keeffe (1991) which gave very similar results to the parameters of Brown (1981) when compared using the type-B structure of $Dy_2Si_2O_7$ (Fleet and Liu 2000).

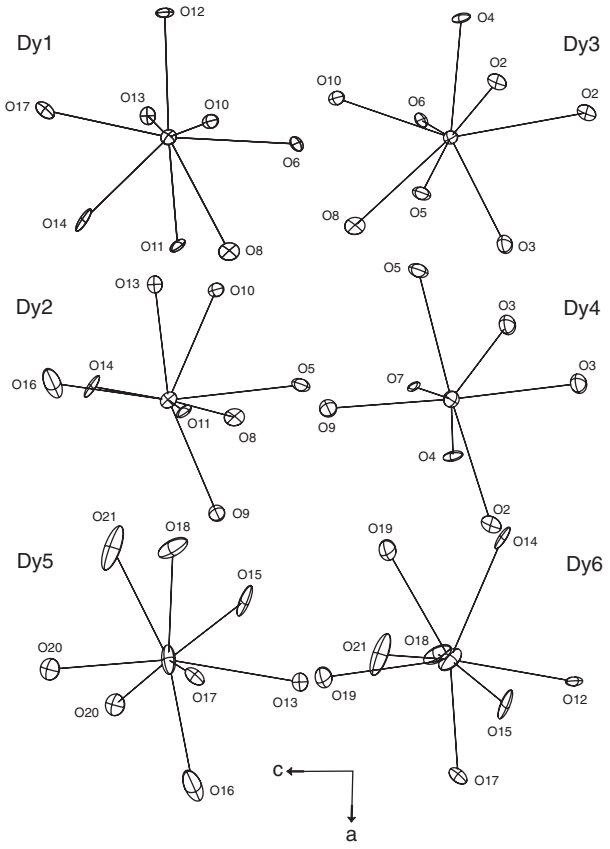

FIGURE 3. Coordination environment of Dy positions in the type-L structure of $Dy_2Si_2O_7$. The displacement ellipsoids are scaled to enclose 50% probability; [010] projection; drawn with *ORTEP*3 (Farrugia 1999).

Data reduction and structure determination

Resolution of the present X-ray structures is limited by the difficulty in making accurate correction for absorption, as well as by the variable diffraction quality of the crystals. The crystal fragments from the quenched high-pressure experiments were few in number, bound by irregular surfaces, and too small for sphere grinding procedures. Although the absorption correction is generally minimized by reducing crystal size, the errors in approximating crystal facets may be proportionally greater for heavy absorbing crystals. In consequence, measurements of crystal polyhedral size and shape required by the analytical correction procedure are semi-quantitative at best for irregularly shaped crystals. For example, absorption correction for crystal xt354 ($Dy_2Si_2O_7$) using the Gaussian analytical method of Coppens et al. (1965; programme DATAP77, Coppens 1997b) did result in somewhat lower R values ($R = 0.042$, w$R = 0.040$, $s = 0.96$) than those reported in Table 1, but R_{int} (0.057) was higher, the anisotropic displacement parameters for O4, O7, O11, and O14 were non-positive definite, and displacement ellipsoids for other O atoms were excessively deformed as well.

The empirical absorption correction procedure in SORTAV uses equivalent reflections for the entire CCD data set indexed by the COLLECT software. It appears to result in a more satisfactory correction than the analytical method for crystals of irregular shape; negative crystal shapes are particularly troublesome for the latter method. SORTAV gives adequate absorption correction for REE disilicates with diorthosilicate structures, using crystals of diverse size and shape (Fleet and Liu 2001). We have recently determined the diorthosilicate structure of type-X $Lu_2Si_2O_7$ (cf. Smolin 1970), obtaining $R = 0.023$, w$R = 0.017$, and $s = 1.04$ for an equant crystal with dimensions $0.025 \times 0.025 \times 0.030$ mm^3 (work in progress). For xt354, the anisotropic displacement parameters for O14 remained non-positive definite using the empirical method, but only when errors were taken into account. A few other anisotropic displacement parameters for O atoms

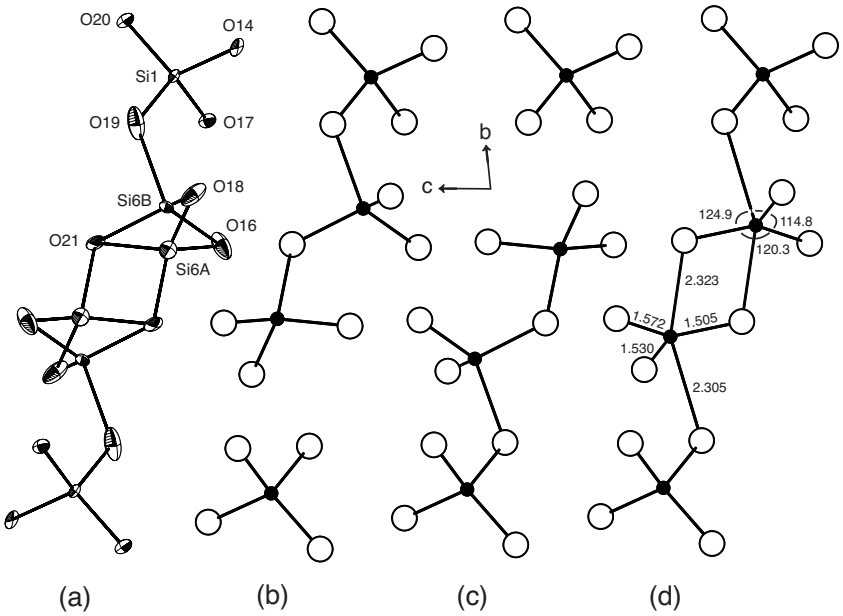

FIGURE 4. (**a**) Chain of corner-, face-, and edge-shared SiO_4 tetrahedra in a (001) strip of disordered sheared structure in type-L $Dy_2Si_2O_7$, showing two Si positions with half occupancy (Si6A and Si6B); (**b**) and (**c**) two possible ways of ordering Si6A and Si6B, resulting in a linear trisilicate $[Si_3O_{10}]^{8-}$ ion and an orthosilicate $[Si4O_4]^{4-}$ ion; and (**d**) the fivefold trigonal bipyramidal coordination, resulting when Si6 with unit occupancy is placed mid-way between Si6A and Si6B. The displacement ellipsoids are scaled to enclose 50% probability; the diagram was drawn with *ATOMS* (Dowty 1995).

TABLE 5. Bond valences for $Dy_2Si_2O_7$ type L (after Brese and O'Keeffe 1991)

	Dy1	Dy2	Dy3	Dy4	Dy5	Dy6	Si1	Si2	Si3	Si4	Si5	Si6A	Si6B	Σ
O1								0.89	0.97					1.86
O2			0.22	0.44				0.98						1.82
			0.18											
O3			0.51	0.09					1.04					2.18
				0.54										
O4			0.54	0.54					1.13					2.21
O5			0.24	0.39	0.43			0.98						2.04
O6	0.36		0.47					1.09						1.92
O7				0.35					0.97		0.78			2.10
O8	0.14	0.41	0.29								0.98			1.82
O9		0.42			0.66					1.07				2.15
O10	0.46	0.24	0.48							0.98				2.14
O11	0.53	0.53									1.03			2.09
O12	0.47					0.30					1.06			1.83
O13	0.48	0.34			0.35					0.93				2.10
O14	0.19	0.38				0.22	1.00							1.79
O15					0.39	0.51				1.00				1.90
O16		0.41			0.46							0.47	0.49	1.83
O17	0.43				0.27	0.43	0.89							2.02
O18					0.58	0.55						0.47	0.60	2.20
O19						0.27	0.99						0.51	2.07
						0.30								
O20					0.43		1.01							1.96
					0.52									
O21					0.14	0.47						0.62	0.52	2.02
												0.27		
Σ	3.06	2.97	3.08	3.05	3.14	3.05	3.89	3.94	4.11	3.98	3.85	1.83	2.12	

were anomalous, but U_{eq} agreed with U_{iso} to within $\pm 1\sigma$ for all O atoms except O15 and O21, for which the agreement was within $\pm 2\sigma$ and $\pm 3\sigma$, respectively. We used isotropic displacement parameters for the Si positions with half occupancy (Si6A, Si6B) and for all of the O atoms in both $Tm_2Si_2O_7$ and $Lu_2Si_2O_7$, since the anisotropic displacement parameters for one or two O atoms in each refinement were non-positive definite. Note that the empirical absorption correction method resulted in similar structure refinements for all three of the presently investigated crystals, which were of different size and shape. Equivalent isotropic displacement parameters generally agree within $\pm 1\sigma$, except for O atoms of or neighboring the sheared strip, which are both anomalously large and variable from one structure to another due to the positional disorder of Si6A and Si6B. Also, the maximum and minimum residual electron densities (Table 1) were located near rare earth cation positions, and are typical of other REE disilicate structures (e.g., Fleet and Liu 2001, 2003; work in progress).

One additional problem is that the diffraction quality of the REE disilicates with linear trisilicate ions (Fleet and Liu 2003; present study) is diminished by decompression effects relative to that of the diorthosilicate disilicates (Fleet and Liu 2001; work in progress). This is related to the greater complexity of the trisilicate structures, as well as local ordering and possible phase transition in the type-L disilicates. Given that diorthosilicates yield generally satisfactory structure refinements, decompression effects likely contributed significantly to the limited resolution of the relatively weak scattering atoms in the type-L structure.

The structure refinements of the Tm and Lu disilicates revealed REE^{3+} cation occupancies <1.0, and corresponding nonstoichiometric formulae of $Tm_{1.97}Si_2O_7$ and $Lu_{1.92}Si_2O_7$, respectively, with the latter in good agreement with the EPMA results. The influence of this nonstoichiometry on structure parameters was not evident, even for Lu4 which had an occupancy of only 0.91. Its origin was unclear as well although, since these crystals were grown in the presence of 5–6 wt% H_2O (Table 1), incorporation of H as $(OH)^-$ is a reasonable possibility.

The type-L structure does not seem to be an "incorrect" structure, as defined by Harlow (1996). We note that: (1) the same structure has been obtained for three isomorphs using crystals of different size and shape (Table 1); (2) the structures of $Dy_2Si_2O_7$, $Tm_2Si_2O_7$, and $Lu_2Si_2O_7$ are similar in respect to structural details (anomalous anisotropic displacements and bond distances, etc.), differing only in the progressive reduction in REE-O distances (and size of $REEO_n$ polyhedra) in the sequence Dy → Tm → Lu; (3) sharp reflections in precession photographs and relatively low errors in unit-cell parameters (Table 1) point to crystals of adequate diffraction quality; (4) superstructure reflections were not detected by the Nonius Kappa CCD diffractometer, which had earlier demonstrated good sensitivity to superstructure reflections in synthetic chlorapatite (Fleet et al. 2000); (5) lacking any evidence of complication in the diffraction patterns, there is no basis for undertaking a dark field TEM or HRTEM study of these crystals; (6) although each anisotropic refinement resulted in a few non-positive definite anisotropic displacement parameters, these were limited in number, sporadic, restricted to atoms that were weak scatterers, and different from one crystal to another; and (7) the low crystal symmetry and restriction of anomalous bond distances to the strip of sheared structure confirm that the half occupancy of Si6A and Si6B is not an artifact of transformation twinning. We recognize that Si6A and Si6B are likely to be, at the very least, locally ordered within the type-L structure. If long-range ordering is present, the associated superstructure reflections are too weak to be detected by the diffractometer used for collection of reflection intensities.

Comparison with other linear trisilicate structures

Figures 1 and 2 show that the strip of type-B structure in type-L $Dy_2Si_2O_7$ is visually equivalent to the type-B structure of $Dy_2Si_2O_7$ (Fleet and Liu 2003) in [100] and [010] projections,

differing only in the orientation of the "structural grain" defined by the structural elements in the latter projection, which is parallel to [101] in type-B and [$\bar{1}$01] in type-L. Equivalent Si and Dy positions in the two structures listed in sequence of L-B are: Si4-Si1, Si5-Si2, Si3-Si3, Si2-Si4, and Dy1-Dy1, Dy3-Dy2, Dy4-Dy3, Dy2-Dy4, respectively. The geometries of corresponding SiO_4 tetrahedra in the type-L and -B structures are closely comparable, including the characteristic long bond to the bridging O atom in one of the terminal tetrahedra, which is 1.718 Å for Si5-O7 in type-L and 1.708 Å for Si2-O4 in type-B, and the small associated bridging-O atom bond angle (Table 6). Moreover, there is striking agreement between the coordination environments of corresponding Dy atoms as viewed in [010] projection (Fig. 3): note that we have included O3 in the coordination environment of Dy4 in the type-L structure although the Dy4-O3 distance of 2.936 Å is relatively long and the corresponding O atom was not included in the coordination environment of the equivalent Dy atom (Dy3) in the type-B structure (Fleet and Liu 2003).

There is a close correspondence between the unit-cell dimensions of the type-L and -B structures of $Dy_2Si_2O_7$ which, in turn, relates to a close correspondence between the dimensions and compositions of the type-B and sheared strips in the type-L structure. For example, a [= 6.5971(3) and 6.6158(2) Å] and b [= 6.6504(2) and 6.6604(2) Å, for type-L and B, respectively] are closely comparable in the two structures and the unit-cell axial angles tend to be complementary [α = 83.791(2) and 94.373(2)°, β = 88.653(2) and 90.836(2)°, and γ = 88.498(2) and 91.512(2)°], but c and V are larger by about x1.5 in the type-L structure [18.0582(6) and 12.0551(4) Å, and 787.2 and 529.4 Å^3, respectively]. Thus, the type-B strip is almost precisely twice as wide as the sheared strip, in agreement with the difference in strip compositions, which are $Dy_8Si_8O_{28}$ and $Dy_4Si_4O_{14}$ per unit cell, respectively. Moreover, in the type-L structure the sheared strip affords structural continuity with the type-B strip in a manner that is very similar to the continuity within the type-B structure itself. The isolated SiO_4 tetrahedron and terminal tetrahedra of the linear trisilicate ion in the type-B structure of $Dy_2Si_2O_7$ are interconnected by Dy1 and Dy4 cations. Similarly, the equivalent large cations in the type-L structure of $Dy_2Si_2O_7$, which are Dy1 and Dy2, respectively, provide continuity between the strips of type-B and sheared structure, as shown in Figure 2, and are seen in this [010] projection to be almost translation-repeated by 2/3[001] to Dy5 and Dy6, respectively. The Si6A and Si1 tetrahedra in the sheared strip are similarly almost translation-repeated by 2/3[001] to the Si5 and Si4 tetrahedra, respectively, in the type-B strip (Fig. 2). In addition, in [100] projection (Fig. 1), the Si6A and Si1 tetrahedra and Dy5 and Dy6 polyhedra in the sheared strip and Si4 and Si5 tetrahedra and Dy2 and Dy1 polyhedra in the type-B strip are spatially and geometrically equivalent to the structural elements providing continuity along the boundaries of panels of $[Si_3O_{10}]^{8-}$ ions and isolated $[SiO_4]$ tetrahedra in the type-B structure of $Dy_2Si_2O_7$ viewed in [100] projection.

Further structural and dimensional correspondence between the type-L and B structures is shown by twinned crystals of type-L $Ho_2Si_2O_7$ and $Tm_2Si_2O_7$ from the piston-cylinder experiments. As in the type-B structure, twin individuals of the $P\bar{1}$ lattice of type-L were related by reflection on (010) and 180° rotation around the **b** axis, and single-crystal diffractometer measurements yielded a dimensionally monoclinic unit cell and space group $C\bar{1}$, which was seemingly a superstructure of the type-L structure. For $Ho_2Si_2O_7$ from experiment PC11, the $C\bar{1}$ unit-cell parameters [a = 33.6351(18), b = 21.2326(10), c = 6.5994(3) Å, and β = 91.9875(28)°] were transformed to $P\bar{1}$ parameters [a = 6.5994(3), b = 6.6294(1), c = 18.0574(13) Å, α = 83.8813(26), β = 88.7661(37), γ = 88.3195(39)°] using a matrix analogous to that derived for the twinned crystal of type-B $Dy_2Si_2O_7$ (Fleet and Liu 2000, 2003). Unfortunately, the reflections collected from the twinned crystal of type-L $Ho_2Si_2O_7$ resulted in an unsatisfactory refinement of the crystal structure, following the procedure used for the twinned crystal of type-B $Dy_2Si_2O_7$. Presumably, this was because the twinned type-L $P\bar{1}$ lattices were not ideally coincident.

TABLE 6. Comparison of bridging-oxygen bond angles in linear trisilicate ion of type B and L structures

Structure type	REE	Bridging-oxygen bond angle (°)	
B	–	Si2-O4-Si3	Si3-O7-Si4
L	–	Si5-O7-Si3	Si3-O1-Si2
B	Gd	121.1	129.5
B	Tb	119.9	129.6
B	Dy	120.3	130.5
B	Ho	118.7	130.2
L	Dy	118.5	130.7
L	Tm	117.4	130.1
L	Lu	115.6	130.8

Linear trisilicate $[Si_3O_{10}]^{8-}$ ions are rare in silicates (e.g., Liebau 1985) and have been reported previously only in the type-B structure of single-REE disilicates, ardennite, $Mn_2^{2+}(Mn^{2+},Ca)_2(AlOH)_4[(Mg,Al,Fe^{3+})OH]_2(As,V)O_4Si_3O_{10}(SiO_4)_2$ (Donnay and Allmann 1968) and kilchoanite ($Ca_6Si_3O_{10}SiO_4$; Taylor 1971), and additionally suggested by Taylor (1971) to be present in the compound $Ca_8Si_5O_{18}$, which can be reorganized to $Ca_8Si_3O_{10}(SiO_4)_2$. Interestingly, the kilchoanite structure is topologically analogous to the type-B structure but has strips of olivine-derivative γ-Ca_2SiO_4 structure alternating with strips of $Ca_4Si_3O_{10}$ composition. Thus, Taylor (1971) predicted a structural series based on the addition of strips of γ-Ca_2SiO_4 structure to the kilchoanite structure. From the foregoing discussion of their topological correspondence, the type-B and sheared strips could be combined in different proportions to give a homologous series of structures based on that of type-L.

Fivefold coordinated Si?

The experimental results of Bocquillon et al. (1977) showing that the type-B structure is adopted by the disilicates of Tm, Yb, and Lu at 7.0 GPa suggest that with increase in pressure the composition field of this structure type is either extended or shifted to higher atomic number (and smaller REE^{3+} cation size). The synthesis experiments discussed in preliminary form in this study show that, for middle- and heavy-REE disilicates, the type-L structure may replace the type-B structure at pressures ranging from <4 to <10 GPa. However, the type-L structure does not have high-pressure characteristics, since type-L and -B polymorphs (e.g., of $Dy_2Si_2O_7$) are similar in respect to coordination of Si and REE, size and distortion of SiO_4 tetrahedra (Table 7) and large cation polyhedra, bridging O atom (Si-O-Si) bond angles (Table 6), and packing density. The increase in density from type-B to type-L $Dy_2Si_2O_7$, calculated with room-pressure

TABLE 7. Size and distortion parameters for SiO_4 tetrahedra in type B and L structures

Structure		Type B strip				Sheared strip		
type	REE	trisilicate ion						
B	-	Si4	Si3	Si2	Si1			
L	-	Si2	Si3	Si5	Si4	Si1	Si6A	Si6B
		Nonbridging O atoms						
B	-	3	2	3	4	–	–	–
L	-	3	2	3	4	3	2	2
		⟨Si-O⟩ (Å)						
B	Dy	1.637	1.625	1.645	1.616	-	-	-
L	Dy	1.630	1.615	1.642	1.626	1.636	1.672	1.667
L	Tm	1.618	1.628	1.637	1.631	1.634	1.679	1.671
L	Lu	1.620	1.624	1.636	1.614	1.629	1.673	1.685
		Polyhedral volume(Å³)						
B	Dy	2.227	2.183	2.254	2.133	–	–	–
L	Dy	2.201	2.145	2.249	2.172	2.230	2.285	2.295
L	Tm	2.143	2.197	2.229	2.194	2.221	2.326	2.307
L	Lu	2.153	2.178	2.227	2.126	2.201	2.311	2.373
		Quadratic elongation[1]						
B	Dy	1.0075	1.0056	1.0092	1.0110	–	–	–
L	Dy	1.0074	1.0051	1.0070	1.0103	1.0048	1.0372	1.0295
L	Tm	1.0100	1.0052	1.0074	1.0100	1.0049	1.0318	1.0287
L	Lu	1.0096	1.0067	1.0065	1.0106	1.0048	1.0276	1.0262
		Bond length distortion ($\times 10^5$)[2]						
B	Dy	16	25	51	35	–	–	–
L	Dy	26	21	76	14	14	462	533
L	Tm	13	28	78	17	13	293	409
L	Lu	12	28	81	13	7	140	373
		Bond angle variance[1]						
B	Dy	33	22	36	42	–	–	–
L	Dy	32	19	28	42	19	112	83
L	Tm	42	19	29	41	20	107	89
L	Lu	40	25	24	42	19	103	83

Notes: 1 = Robinson et al. (1971); 2 = Fleet (1976).

measurements, is only 1.4% and significantly less than the increase of 12–14% from the room-pressure type-G $Nd_2Si_2O_7$ and $Sm_2Si_2O_7$, type-F $Eu_2Si_2O_7$, and type-E $Gd_2Si_2O_7$ structures to the quenched 10 GPa type-K structures for these REE disilicates (Fleet and Liu 2001).

One explanation for this apparent discrepancy in density is that the type-L structure of $Dy_2Si_2O_7$, $Tm_2Si_2O_7$, and $Lu_2Si_2O_7$ formed while quenching the high-pressure experiments from a denser precursor phase, topologically similar to the type-L phase but with some Si cations in higher coordination. The logical candidates for this pressure-induced change in coordination of Si are Si6A and Si6B, which are present as half-occupied pairs of face-sharing tetrahedra in the type-L structure, and would order to give Si (Si6) in fivefold trigonal bipyramidal coordination with unit occupancy at high pressure, as suggested in Figure 4d. In this hypothetical high-pressure REE disilicate structure, two trigonal bipyramids share a common edge, resulting in the kinked (<180°) axial O-Si-O bond angle that is typical of this coordination in organosilicates (Tacke et al. 1999, 2000). The three equatorial Si-O distances are significantly shorter and the two axial Si-O distances significantly longer than the corresponding bond distances in the organosilicate structures, but this could be attributed to relaxation of the trigonal bipyramidal cluster of O atoms in the type-L structure to accommodate the tetrahedral geometry required by Si6A and Si6B.

Transformation to the type-L phase during quenching of the pressure requires the breaking of only one Si-O bond per $Si6O_5$ trigonal bipyramid and the displacement of the Si6 atom into one of the two possible tetrahedral environments. In this respect, the formation of the type-L structure from the hypothetical nonquenchable high-pressure phase is analogous to the formation of triclinic $CaSi_2O_5$ with pentacoordinated square pyramidal Si by decompression of the nonquenchable phase monoclinic $CaSi_2O_5$. This transition was predicted by Kanzaki et al. (1991) and Angel et al. (1996) from experiments at about 11 GPa, and confirmed to occur at a pressure between 0.17 and 0.205 GPa by Angel (1997). Relaxation of the high-pressure monoclinic $CaSi_2O_5$ structure at the transition pressure results in the stretching of one Si-O bond in every second SiO_6 octahedron to a non-bonded distance of 2.83 Å. A closer analogy to the present situation is afforded by the high-pressure silicate $CaAl_4Si_2O_{11}$ (Gautron et al. 1997, 1999). The face-sharing Si(Al) tetrahedra in this hexagonal Ba-ferrite-type compound are directly equivalent to $Si6AO_4$ and $Si6BO_4$ in the type-L structure, and the possibility of their pressure-induced transformation to a single fivefold trigonal bipyramidal coordination is supported by fivefold-coordinated V in the analogous vanadium oxides (Kanke et al. 1992). We note that the fivefold-coordinated trigonal bipyramidal group is well known for nonrigid behavior in coordination compounds; in fact, nonrigidity is the rule for five-coordinate complexes rather than the exception (Cotton and Wilkinson 1988) and there are numerous examples of nonquenchable behavior involving high-pressure inorganic structures with cations in uncommon high coordinations (e.g., Hyde and Andersson 1989).

The distortion of the $Si6AO_4$ and $Si6BO_4$ tetrahedra from ideal geometry (Table 7) is seemingly consistent with decomposition of a SiO_5 trigonal bipyramid, combined with positional disorder and partial relaxation to room pressure. Each of these tetrahedra has one long (1.78–1.85 and 1.85–1.87 Å, respectively) and one short (1.54–1.62 and 1.55–1.59 Å, respectively) Si-O distance (Table 3). The more anomalous of these distances fall outside of the Si-O bond distance range for tetrahedral Si in silicate structures in general (e.g., Baur 1970) and, thus, probably represent space-averaged atomic positions rather than actual bonded distances. Evidently, considerable positional disorder remains frozen in within the sheared-strip region of the pressure-quenched structure. In summary, the half occupancy of the Si6A and Si6B positions, low crystal symmetry ($P\bar{1}$) and stretched Si6A-O21 and Si6B-O19 bond distances would seem to be evidence favoring formation of the type-L structure by transformation from a high-pressure precursor phase. The inferred high-pressure structure and transformation mechanism require confirmation by in situ diffraction measurements, but we recognize that this might be experimentally difficult if the diffraction patterns of the two phases are very similar.

ACKNOWLEDGMENTS

We thank R. Luth for the high-pressure synthesis, M. Jennings and the Department of Chemistry for collection of reflection intensities, Y. Thibault and M. Liu for assistance with EPMA, two reviewers for helpful comments, and the Natural Sciences and Engineering Research Council of Canada for financial support.

REFERENCES CITED

Angel, R.J. (1997) Transformation of fivefold-coordinated silicon to octahedral silicon in calcium silicate, $CaSi_2O_5$. American Mineralogist, 82, 836–839.
Angel, R.J., Ross, N.L., Seifert, F., and Fliervoet, T.F. (1996) Structural characteriza-

tion of pentacoordinate silicon in a calcium silicate. Nature, 384, 441–444.
Baur, W.H. (1970) Bond length variation and distorted coordination polyhedra in inorganic crystals. Transactions of the American Crystallographical Association, 6, 129–155.
Bocquillon, G., Chateau, C., Loriers, C., and Loriers, J. (1977) Polymorphism under pressure of the disilicates of the heavier lanthanoids (thulium, ytterbium, lutetium). Journal of Solid State Chemistry, 20, 135–141.
Bohlen, S.R. (1984) Equilibria for precise pressure calibration and a frictionless furnace assembly for the piston-cylinder apparatus. Neues Jahrbuch für Mineralogie, Monatshefte, 9, 404–412.
Bohlen, S.R. and Boettcher, A.L. (1982) The quartz - coesite transformation: a precise determination and the effects of other components. Journal of Geophysical Research, 87, 7073–7078.
Brese, N.E. and O'Keeffe, M. (1991) Bond-valence parameters for solids. Acta Crystallographica, B47, 192–197.
Brown, I.D. (1981) The bond-valence method: An empirical approach to chemical structure and bonding. In M. O'Keeffe and A. Navrotsky, Eds., Structure and bonding in crystals II, p. 1–30. Academic Press, New York.
Christensen, A.N. (1994) Investigation by the use of profile refinement of neutron powder diffraction data of the geometry of the $[Si_2O_7]^{6-}$ ions in the high temperature phases of rare earth disilicates prepared from the melt in crucible-free synthesis. Zeitschrift für Kristallographie, 209, 7–13.
Christensen, A.N. and Hazell, R.G. (1994) X-ray crystallographic study of $Ce_2Si_2O_7$. Acta Chemica Scandinavica, 48, 1012–1014.
Christensen, A.N., Hazell, R.G., and Hewat, A.W. (1997a) Synthesis, crystal growth and structure investigations of rare-earth disilicates and rare-earth oxyapatites. Acta Chemica Scandinavica, 51, 37–43.
Christensen, A.N., Jensen, A.F., Themsen, B.K., Hazell, R.G., Hanfland, M., and Dooryhee, E. (1997b) Structure investigations of the high-temperature phases of $La_2Si_2O_7$, $Gd_2Si_2O_7$ and $Sm_2Si_2O_7$. Acta Chemica Scandinavica, 51, 1178–1185.
Coppens, P. (1997a) LINEX77. State University of New York, Buffalo, U.S.A.
——— (1997b) DATAP77. State University of New York, Buffalo, U.S.A.
Coppens, P., Leiserowitz, L., and Rabinovich, D. (1965) Calculation of absorption corrections for camera and diffractometer data. Acta Crystallographica, 18, 1035–1038.
Cotton, F.A. and Wilkinson, G. (1988). Advanced Inorganic Chemistry, 5th Ed. Wiley, New York.
Dias, H.W., Glasser, F.P., Gunwardane, R.P., and Howie, R.A. (1990) The crystal structure of δ-yttrium pyrosilicate, δ-$Y_2Si_2O_7$. Zeitschrift für Kristallographie, 191, 117–123.
Donnay, G. and Allmann, R. (1968) Si_3O_{10} groups in the crystal structure of ardennite. Acta Crystallographica, B24, 845–855.
Dowty, E. (1995) ATOMS for Windows. Version 3.1. Shape Software, 521 Hidden Valley Road, Kingsport, TN 37663, U.S.A.
Farrugia, L.J. (1999) Ortep-3 for Windows. University of Glasgow, U.K.
Felsche, J. (1970a) Polymorphism and crystal data of the rare-earth disilicates of type $R.E._2Si_2O_7$. Journal of the Less-Common Metals, 21, 1–14.
——— (1970b) The crystal structure of α-$Pr_2Si_2O_7$. Naturwissenschaften, 57, 452.
——— (1970c) The crystal structure of β-$Pr_2Si_2O_7$. Naturwissenschaften, 57, 669–670.
——— (1971) The crystal structures of the dimorphic rare earth disilicate, $Pr_2Si_2O_7$. Zeitschrift für Kristallographie, 133, 364–385.
——— (1972) A new silicate structure containing linear $[Si_3O_{10}]$ groups. Naturwissenschaften, 59, 35–36.
Fleet, M.E. (1976) Distortion parameters for coordination polyhedra. Mineralogical Magazine, 40, 531–533.
——— (1998) Sodium heptasilicate: A high-pressure silicate with six-membered rings of tetrahedra interconnected by SiO_6 octahedra: $(Na_8Si[Si_6O_{18}])$. American Mineralogist, 83, 618–624.
Fleet, M.E. and Liu, X. (2000) Structure and complex twinning of dysprosium disilicate ($Dy_2Si_2O_7$), type B. Acta Crystallographica, B56, 940–946.
——— (2001) High-pressure rare earth disilicates $REE_2Si_2O_7$ (REE = Nd, Sm, Eu, Gd): type K. Journal of Solid State Chemistry, 161, 166–172.
——— (2003) Rare earth disilicates $R_2Si_2O_7$ (R = Gd, Tb, Dy, Ho): type B. Zeitschrift für Kristallographie, 218, 795–801.
Fleet, M.E., Liu, X., and Pan, Y. (2000) Rare earth elements in chlorapatite $[Ca_{10}(PO_4)_6(Cl)_2]$: Uptake, site preference and degradation of monoclinic structure. American Mineralogist, 85, 1437–1446.
Gautron, L., Fitz Gerald, J.D., Kesson, S.E., Eggleton, R.A., and Irifune, T. (1997) Hexagonal Ba-ferrite: a good model for the crystal structure of a new high-pressure phase $CaAl_4Si_2O_{11}$? Physics of the Earth and Planetary Interiors, 102, 223–229.
Gautron, L., Angel, R.J., and Miletich, R. (1999) Structural characterisation of the high-pressure phase $CaAl_4Si_2O_{11}$. Physics and Chemistry of Minerals, 27, 47–51.
Greis, O., Bossemeyer, H.G., Greil, P., Breidenstein, B., and Haase, A. (1991) Structural data of the monoclinic high-temperature G-form of $La_2Si_2O_7$ from X-ray powder diffraction. Materials Science Forum, 79–82, 803–808.
Harlow, R.L. (1996) Troublesome crystal structures: Prevention, detection, and resolution. Journal of Research of the National Institute of Standards and Technology, 101, 327–339.
Hazen, R.M., Downs, R.T., and Finger, L.W. (1996) High-pressure framework silicates. Science, 272, 1769–1771.
Hyde, B.G. and Andersson, S. (1989) Inorganic Crystal Structures. Wiley, New York.
Ibers, J.A. and Hamilton, W.C. Eds. (1974) International Tables for X-ray Crystallography, vol. IV. Kynoch Press, Birmingham, U.K.
Kanke, Y., Kato, K., Takayama-Muromachi, E., and Isobe, M. (1992) Structures of SrV_6O_{11} and NaV_6O_{11}. Acta Crystallographica, C48, 1376–1380.
Kanzaki, M., Stebbins, J.F., and Xue, X. (1991) Characterization of quenched high pressure phases in $CaSiO_3$ system by XRD and ^{29}Si NMR. Geophysical Research Letters, 18, 463–466.
Liebau, F. (1985) Structural Chemistry of Silicates. Berlin, Springer-Verlag.
Liu, X. and Fleet, M.E. (2002) High-pressure synthesis of a La orthosilicate and Nd, Gd, and Dy disilicates. Journal of Physics: Condensed Matter, 14, 11223–11226.
Loriers, J., Bocquillon, G., Chateau, C., and Colaïtis, D. (1977) Rare earth disilicates $Ln_2Si_2O_7$: data on their new crystalline X form and their polymorphism under pressure. Materials Research Bulletin, 12, 403–413.
Müller-Bunz, H. and Schleid, T. (2000) Über den H- und A-typ von $La_2[Si_2O_7]$. Zeitschrift für Anorganische und Allgemeine Chemie, 626, 2549–2556.
——— (2002) $La_2Si_2O_7$ im I-typ: Gemäß $La_6[Si_4O_{13}][SiO_4]_2$ kein echtes lanthandisilicat. Zeitschrift für Anorganische und Allgemeine Chemie, 628, 564–569.
Robinson K., Gibbs G.V., and Ribbe P.H. (1971) Quadratic elongation: A quantitative measure of distortion in coordination polyhedra. Science, 172, 567–570.
Sewell, D.A., Love, G., and Scott, V.D. (1985) Universal correction procedure for electron-probe microanalysis: I. Measurement of x-ray depth distributions in solids. Journal of Physics D: Applied Physics, 18, 1233–1243.
Siemens (1993) SHELXTL PC (Version 4.1). Siemens Analytical X-ray Instruments, Inc. Madison, Wisconsin 53719, U.S.A.
Smolin, Yu.I. (1970) Determination of the crystal structure of erbium pyrogermanate, $Er_2Ge_2O_7$. Soviet Physics Crystallography, 15, 36–39.
Smolin, Yu.I. and Shepelev, Yu.F. (1970) The crystal structures of the rare earth pyrosilicates. Acta Crystallographica, B26, 484–492.
Smolin, Yu.I., Shepelev, Yu.F., and Butikova, I.K. (1970) The crystal structure of the low-temperature form of samarium pyrosilicate, $Sm_2Si_2O_7$. Soviet Physics Crystallography, 15, 214–219.
Stebbins, J.F. and McMillan, P. (1989) Five- and six-coordinated Si in $K_2Si_4O_9$ glass quenched from 1.9 GPa and 1200°C. American Mineralogist, 74, 965–968.
Tacke, R., Pfrommer, B., Pülm, M., and Bertermann, R. (1999) New chiral zwitterionic λ^5Si-silicates with an SiO_5 or SiO_4C framework: Syntheses, crystal structures, and properties. European Journal of Inorganic Chemistry, 5, 807–816.
Tacke, R., Burschka, C., Richter, I., Wagner, B., and Willeke, R. (2000) Pentacoordinate silicon compounds with SiO_5 skeletons containing SiOH or SiOSi groups: Derivatives of the pentahydroxosilicate(1–) anion $[Si(OH)_5]^-$ and its anhydride $[(HO)_4Si\text{-}O\text{-}Si(OH)_4]^{2-}$. Journal of the American Chemical Society, 122, 8480–8485.
Tacke, R., Bertermann, R., Dannappel, O., Neugebauer, R.E., Pülm, M., and Willeke, R. (2001) Monocyclic zwitterionic λ^5Si-silicates with an SiO_2FC_2 framework: Syntheses and structural characterization in the solid state and in solution. Inorganic Chemistry, 40, 2520–2527.
Taylor, H.F.W. (1971) The crystal structure of kilchoanite, $Ca_6(SiO_4)(Si_3O_{10})$, with some comments on related phases. Mineralogical Magazine, 38, 26–31.
Turley, J.W. and Boer, F.P. (1968) Structural studies of pentacoordinate silicon. I. Phenyl-(2,2',2"-nitrilotriethoxy) silane. Journal of the American Chemical Society, 90, 4026–4030.
Walter, M.J., Thibault, Y., Wei, K., and Luth, R.W. (1995) Characterizing experimental pressure and temperature conditions in multi-anvil apparatus. Canadian Journal of Physics, 73, 273–286.
Warren, M.C., Redfern, S.A.T., and Angel, R. (1999) Change from sixfold to fivefold coordination of silicate polyhedra: Insights from first-principles calculations of $CaSi_2O_5$. Physical Review, B59, 9149–9154.
Wentzcovitch, R.M., da Silva, C., Chelikowsky, J.R., and Binggeli, N. (1998) A new phase and pressure induced amorphization in silica. Physical Review Letters, 80, 2149–2152.

Manuscript received March 27, 2003
Manuscript accepted September 17, 2003
Manuscript handled by Thomas Duffy